Metal Ions Differentially Influence the Aggregation and Deposition of Alzheimer's β-Amyloid on a Solid Template†

Chanki Ha,‡ Jungki Ryu,§ and Chan Beum Park*,‡,§

Science and Engineering of Materials Interdisciplinary Program, Arizona State University, Tempe, Arizona 85287, and Department of Materials Science and Engineering, Korea Advanced Institute of Science and Technology, 373-1 Guseong-dong Yuseong-gu, Daejeon, Republic of Korea

Received January 2, 2007; Revised Manuscript Received March 18, 2007

ABSTRACT: The abnormal deposition and aggregation of β-amyloid (Aβ) on brain tissues are considered to be one of the characteristic neuropathological features of Alzheimer's disease (AD). Environmental conditions such as metal ions, pH, and cell membranes are associated with Aβ deposition and plaque formation. According to the amyloid cascade hypothesis of AD, the deposition of Aβ42 oligomers as diffuse plaques in vivo is an important earliest event, leading to the formation of fibrillar amyloid plaques by the further accumulation of soluble Aβ under certain environmental conditions. In order to characterize the effect of metal ions on amyloid deposition and plaque growth on a solid surface, we prepared a synthetic template by immobilizing Aβ oligomers onto a *N*-hydroxysuccinimide ester-activated solid surface. According to our study using ex situ atomic force microscopy (AFM), Fourier transform infrared spectroscopy (FT-IR), and thioflavin T (ThT) fluorescence spectroscopy, Cu^{2+} and Zn^{2+} ions accelerated both Aβ40 and Aβ42 deposition but resulted only in the formation of "amorphous" aggregates. In contrast, Fe^{3+} induced the deposition of "fibrillar" amyloid plaques at neutral pH. Under mildly acidic environments, the formation of fibrillar amyloid plaques was not induced by any metal ion tested in this work. Using secondary ion mass spectroscopy (SIMS) analysis, we found that binding Cu ions to Aβ deposits on a solid template occurred by the possible reduction of Cu ions during the interaction of Aβ with Cu^{2+}. Our results may provide insights into the role of metal ions on the formation of fibrillar or amorphous amyloid plaques in AD.

Amyloid deposition, which occurs as a result of the conformational change of soluble β-amyloid (Aβ)[1] peptides into insoluble amyloid plaques on a surface, is considered one of the key pathological processes in Alzheimer's disease (AD) (*1*). Recently, there has been growing interest in the role of metal ions as a driving force to modulate the precipitation of soluble Aβ (*2*−*4*). Metal ions such as Cu^{2+}, Fe^{3+}, and Zn^{2+} were found in high concentrations (∼400, ∼950, and ∼1100 μM, respectively) within the core and periphery of senile plaque deposits (*2*, *5*).

Previous studies had mainly focused on the morphological properties of Aβ aggregates and the kinetics of Aβ aggregation in the "free solution" phase. Recent reports indicate that Aβ deposition on the "surface", rather than Aβ aggregation under free solution conditions, is more physiologically relevant (*6*−*8*). In vivo Aβ deposition as amyloid plaques takes place predominantly on the membrane of neuronal cells and in the walls of cerebral blood vessels (*9*, *10*). Thus, the interaction with a solid surface can be an important environmental factor that can influence amyloid deposition in vivo, leading to Aβ conformational changes onto predeposited Aβ plaques.

In our recent work, we successfully simulated the aggregation and deposition process of Aβ peptides by using a solid template that was prepared through the immobilization of oligomeric Aβ seeds onto a *N*-hydroxysuccinimide ester- (NHS-) activated solid surface (*11*). The study demonstrated that the interaction between human Aβ and the template surface coated with Aβ oligomers can induce a conformational change and lead to the growth of amyloid fibrils on the template surface. While the use of a "natural" amyloid template to study amyloid deposition is extremely difficult and cumbersome, amyloid deposition and plaque growth could be studied more efficiently by using the "synthetic" amyloid template.

Here we report the influence of Cu^{2+}, Fe^{3+}, and Zn^{2+} ions on the aggregation and deposition of Aβ on the synthetic solid template system. Both Aβ40 and Aβ42 peptides were tested to compare the effect of different types of amyloid monomers on metal ion-induced amyloid deposition. Properties of amyloid deposits formed on the synthetic template were investigated by multiple analytical tools: ex situ atomic force microscopy (AFM), Fourier transform infrared

† This study was supported by grants from the National Institutes of Health (1R21AG024114-01A2) and the Korea Research Foundation (KRF-2006-D00078).

* To whom correspondence should be addressed. Phone: +82-42-869-3340. Fax: +82-42-869-3310. E-mail: parkcb@kaist.ac.kr.

‡ Arizona State University.

§ Korea Advanced Institute of Science and Technology.

[1] Abbreviations: ThT, thioflavin T; AFM, atomic force microscopy; FT-IR, Fourier transform infrared; NHS, *N*-hydroxysuccinimide ester; AD, Alzheimer's disease; Aβ, β-amyloid; BSA, bovine serum albumin; APTS, (3-aminopropyl)triethoxysilane; DSC, *N*,*N*′-disuccinimidyl carbonate; HFIP, 1,1,1,3,3,3-hexafluoro-2-propanol; SIMS, secondary ion mass spectroscopy.

10.1021/bi7000032 CCC: $37.00 © 2007 American Chemical Society
Published on Web 04/25/2007

(FT-IR) spectroscopy, thioflavin T- (ThT-) induced fluorescence, and secondary ion mass spectroscopy (SIMS).

EXPERIMENTAL PROCEDURES

Materials. Human amyloid-β (Aβ) Aβ42 and Aβ40 were obtained from rPeptide Co. (Athens, GA). Bovine serum albumin (BSA), (3-aminopropyl)triethoxysilane (APTS), *N*,*N*′-disuccinimidyl carbonate (DSC), 1,1,1,3,3,3-hexafluoro-2-propanol (HFIP), $CuCl_2 \cdot 2H_2O$, and $FeCl_3$ were purchased from Sigma-Aldrich (St. Louis, MO). $ZnCl_2$ was obtained from EMD Chemicals Inc. (Gibbstown, NJ). Micro-cover glasses were obtained from VWR Scientific (West Chester, PA).

Preparation of Aβ Solution with or without Metal Ions. To get a uniform, monomeric Aβ42 or Aβ42, lyophilized peptides were first solubilized in 100% HFIP, followed by sonication in a water bath for 3 min. Then, the peptide solution was aliquoted in sterile microcentrifuge tubes. After the HFIP solvents were evaporated in a vacuum using Corning Pyrex brand vacuum desiccators (Fisher Scientific International Inc.), the remaining peptide film was stored at −20 °C. Immediately prior to use, the peptide was dissolved in dimethyl sulfoxide (Me_2SO) and diluted with phosphate-buffered saline (PBS) or a 20 mM Tris buffer in the presence or absence of indicated substances, pH 7.4, to a required concentration. All metal ions were dissolved in the 20 mM Tris buffer.

Surface Treatment for the Solid Template. Micro-cover glasses were chemically treated for the covalent attachment of Aβ oligomer seeds to a glass slide. The surface of the glass slides was treated with a piranha solution of 70% H_2SO_4:30% H_2O_2 (7:3 v/v) for more than 12 h, rinsed with deionized water, and dried by N_2. Subsequent treatment of the slides was carried out with a 3% solution of APTS in ethanol/water (95:5 v/v) for 1 h. The aminopropylated glass slides were placed in 100% ethanol and cured at 110 °C for 1 h. The slides were cooled at room temperature and washed with 95% ethanol. The activation of the glass surfaces with a *N*-hydroxysuccinimide ester (NHS) was obtained by incubating the slides in a 20 mM DSC solution in a sodium bicarbonate buffer (50 mM, pH 8.5) for 3 h at room temperature. After incubation, the slides were washed with deionized water and dried with N_2.

Preparation of the Solid Template and Aβ Deposition on the Template. The preparation of a solid template was carried out as described in our previous work (*11*). Freshly prepared Aβ42 or Aβ40 (30 μM) in a pH 7.4 PBS buffer containing 5% Me_2SO (v/v) was incubated for 12 h at 37 °C. A 7 μL (AFM samples) or 30 μL (SIMS and ThT fluorescence samples) aliquot of the 12 h preincubated Aβ oligomers was uniformly placed onto a NHS-activated glass slide. After a few minutes of incubation, the remaining solution on the glass was blown off by N_2. The solid template, immobilized Aβ oligomers on a solid surface, was transferred to a solution of 0.1% BSA in a 50 mM phosphate buffer (pH 7.5) to block the remaining functionalities. Aβ oligomers weakly bound to the template were removed by washing the template with a 50 mM phosphate buffer (pH 7.5) for 1 h. The template was then washed with deionized water for 45 min and dried with N_2. The dried template was further incubated in freshly prepared Aβ42 (6 μM) or Aβ40 (30 μM) in 20 mM Tris buffer (pH 7.4) containing 5% Me_2SO with or without metal ions at 37 °C. After incubation, the solid samples were cleaned with deionized water and dried with N_2 for further analysis.

Ex Situ Atomic Force Microscopy (AFM). The visualization of Aβ deposits grown on a solid template (4.5 mm × 7 mm) was performed using ex situ AFM. The surface of the solid samples was scanned using a Nanoscope III Multimode AFM (Digital Instruments Inc.) under ambient conditions. Each image was acquired in the tapping mode and under the following conditions: scan rate, 1−2 Hz; an "E" scanner; resonant frequency range of AFM tips, 306−444 kHz; number of pixels, 512 × 512. The quantitative analysis of AFM images was achieved in terms of the volume and height distributions of the Aβ deposits using SPIP software (Image Metrology). To obtain representative images in each case, different samples and five spots in the entire surface areas were scanned.

Reflectance Fourier Transform Infrared (FT-IR) Spectroscopy. Samples were prepared for FT-IR analysis by incubating a solid template (4.5 mm × 7 mm) in a solution containing Aβ42 (6 μM) dissolved in 20 mM Tris buffer (pH 7.4) containing 5% Me_2SO with or without metal ions at 37 °C for 24 h. After incubation, the samples were cleaned and dried before FI-IR measurements were taken. Solid samples were directly placed on a rounded diamond crystal. IR measurements of the solid samples were preformed on a Nicolet Nexus 470 spectrometer (Thermo Nicolet Corp, Madison, WI) equipped with an attenuated total reflection (ATR) accessory. Absorbance spectra of different Aβ samples were collected at a resolution of 4.0 cm^{-1} by subtracting the background spectrum of a plain glass from the sample spectra.

Thioflavin T- (ThT-) Induced Fluorescence Analysis. The formation of amyloid plaques on a solid template in the absence and presence of metal ions was quantitatively characterized by ThT-induced fluorescence. A solid template (8 mm × 18 mm) was incubated in a freshly prepared 6 μM Aβ42 solution with or without metal ions at 37 °C for 24 h. The Aβ42 solution was prepared by dissolving Aβ42 peptides into 20 mM Tris buffer (pH 7.4) with 5% Me_2SO. After incubation, the template samples were put diagonally into the 10 mm long path of a quartz cuvette containing 2 mL of 50 μM ThT solution in a Tris buffer (pH 8, 20 mM). The fluorescence analysis was performed with a spectrofluorometer (Model RF5301; Shimadzu Co.) by measuring emission intensities at 482 nm with excitation at 450 nm. Each measurement was done in triplicate. The average and standard deviation were calculated for data analysis.

Secondary Ion Mass Spectroscopy (SIMS) Analysis. The Cu ion presence of Cu^{2+}-induced Aβ42 deposits (1 cm × 1 cm) was characterized using SIMS (CAMELA IMS-3f). A primary ion (O^-) beam at an impact energy of 12.64 keV sputtered the sample surface in the vacuum chamber. Secondary ions generated from the top few monolayers of the sample were analyzed by either an electron multiplier or a faraday cup. Secondary ion images of Cu^{2+}-induced Aβ42 deposits and a plain glass were compared to find out the metal component of Cu^{2+}-induced Aβ42 deposits on a glass template.

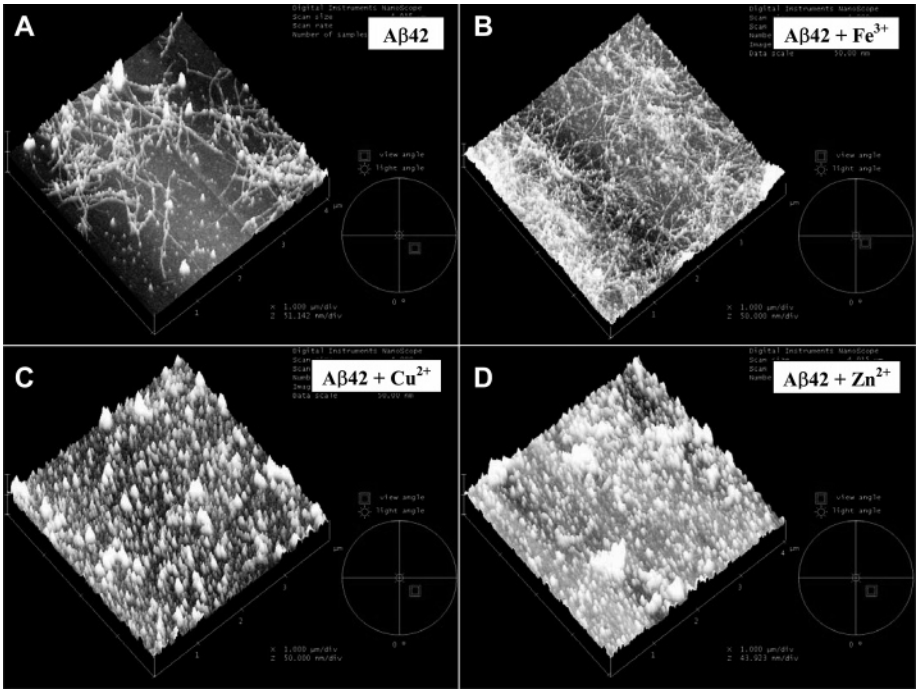

FIGURE 1: Representative AFM images of Aβ42 deposits formed on a solid template in the absence or presence of metal ions. The Aβ42 deposits were obtained by incubating freshly prepared Aβ42 (6 μM) in a 20 mM Tris buffer containing 5% Me_2SO (v/v) (A) without metal ions, (B) with 100 μM $FeCl_3$, (C) with 100 μM $CuCl_2$, or (D) with 100 μM $ZnCl_2$ at 37 °C for 24 h. The template was prepared by immobilizing 12 h preincubated Aβ42 (30 μM) in a pH 7.4 PBS buffer containing 5% Me_2SO (v/v) at 37 °C on an NHS-activated solid surface.

RESULTS AND DISCUSSION

Effect of Metal Ions on Aβ42 Aggregate Formation on a Synthetic Template. To investigate the effect of metal ions on Aβ aggregate formation on a solid template, we prepared a synthetic template by immobilizing Aβ42 oligomers on an NHS-activated solid surface. According to an AFM analysis of the immobilized seeds, the average z-height of the seeds was in the range of 4 ± 2 nm (data not shown), which indicates that the seeds consisted of Aβ oligomeric species. The solid template was incubated in a freshly prepared Aβ42 solution in the presence of metal ions, followed by the analysis of the template surface with ex situ AFM. Figure 1 shows the morphologies of Aβ deposits that formed on the surface after a 24 h incubation period in the presence of each metal ion. As a control experiment, a solid template was incubated in a freshly prepared Aβ42 solution in the absence of metal ion, in which case most of the aggregates that formed on the template surface were found to have "fibrillar" morphology (Figure 1A). This observation suggests that our synthetic template can induce the conformational change of Aβ42 dissolved in the incubation solution, leading to the formation of fibrillar plaques on the template surface. When a template was incubated in a Aβ42 solution containing Fe^{3+}, much denser aggregates with fibrillar shape were observed on the template surface (Figure 1B). In contrast, no fibrils were observed by Aβ42 incubated in the presence of either Zn^{2+} or Cu^{2+}, in which case only spherical or nonfibrillar "amorphous" deposits were found (Figure 1C,D). These observations suggest that Fe^{3+} can be one of the key mediating factors inducing fibrillar β-sheet amyloid deposition, but the interaction of Zn^{2+} or Cu^{2+} with Aβ42 may inhibit the formation of amyloid aggregates in fibrillar form.

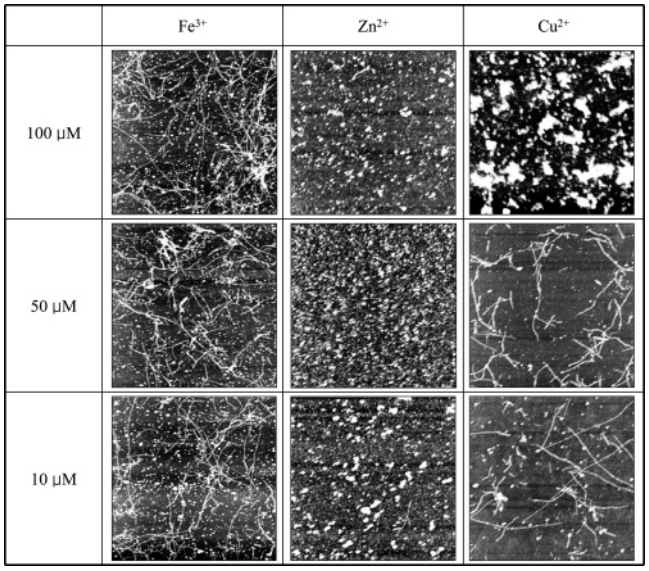

FIGURE 2: Effect of metal ion concentration (100, 50, 10 μM) on template-directed Aβ42 aggregation and deposition. The conditions for the template preparation and the AFM analysis were the same as in Figure 1. The size of each AFM image is 5×5 μm.

To investigate the effect of metal ion concentration on the template-directed Aβ42 aggregation and deposition, we co-incubated Aβ42 monomers with Fe^{3+}, Zn^{2+}, or Cu^{2+} at different concentrations (10, 50, 100 μM) in the presence of solid template. As shown in Figure 2, the total amount of aggregates slightly decreased with the decreasing amount of metal ion in the incubation solution. In the case of Fe^{3+} or Zn^{2+}, the morphologies of aggregates formed on the template surface were similar regardless of their concentrations. In contrast, Cu^{2+} did not induce amorphous deposits any longer at lower concentrations of 10 or 50 μM in the

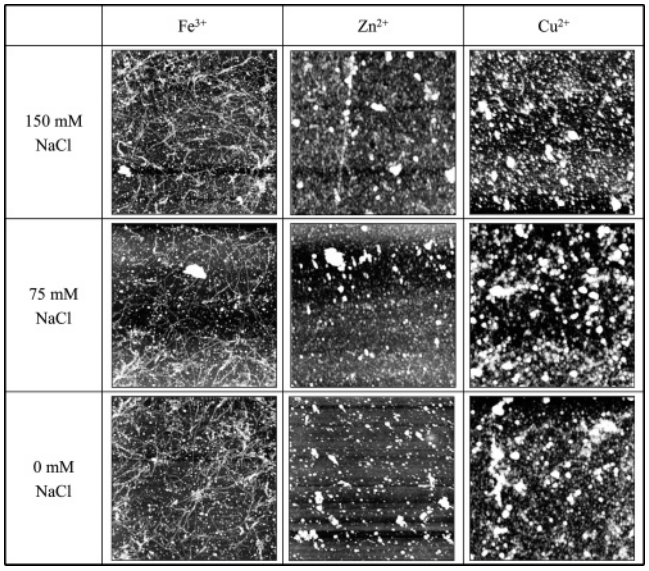

FIGURE 3: Effect of NaCl concentration (150, 75, 0 mM) on the aggregation and deposition of Aβ42 on a solid template. The Aβ42 deposits were obtained by incubating a freshly prepared Aβ42 (6 μM) in 20 mM Tris buffer containing 5% Me_2SO (v/v) in the presence 100 μM metal ions at 37 °C for 24 h. The size of each AFM image is 5 × 5 μm.

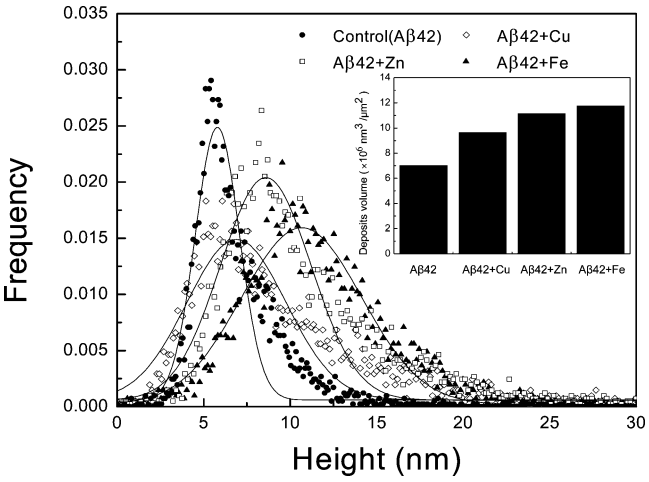

FIGURE 4: Quantitative analysis of AFM images shown in Figure 1. The data acquired by using SPIP software were fitted with Gaussian curves. Inset: Total volume of Aβ42 deposits or Aβ42 deposits induced by different metal ions on the solid surface. All data points were summed to measure the volume of Aβ42 deposits on a template.

incubation solution. Those results indicate that Zn^{2+} induces the amorphous aggregation of Aβ42 on the solid template in much higher strength than Cu^{2+}.

To observe the effect of ionic strength, we carried out the template-directed Aβ42 aggregation in a solution containing NaCl (0, 75, 150 mM) and metal ion (100 μM). According to our analysis with AFM (Figure 3), the presence of NaCl did not change the morphology of aggregates formed on the template surface; i.e., Cu^{2+} or Zn^{2+} resulted only in the formation of nonfibrillar, amorphous aggregates while Fe^{3+} induced the deposition of fibrillar amyloid plaques in the presence or absence of NaCl. The total amount of metal ion-induced aggregates formed on the template surface was also not significantly affected by the presence of NaCl. According to Huang et al. (*12*), Zn^{2+}-induced Aβ aggregation was

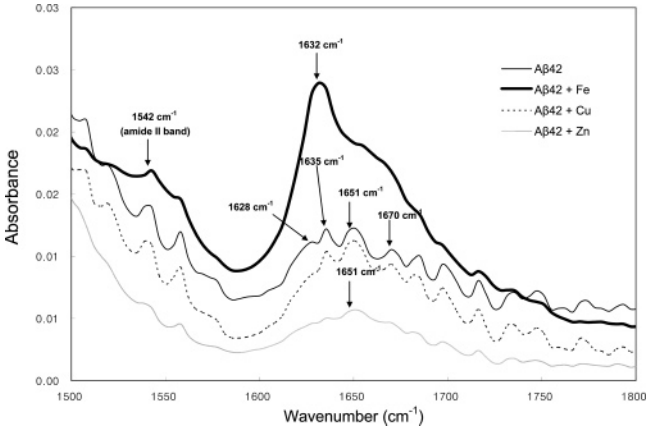

FIGURE 5: FT-IR spectra of Aβ42 deposits induced by different metal ions. A freshly prepared 6 μM Aβ42 solution in the absence or presence of 100 μM Zn^{2+}, Cu^{2+}, or Fe^{3+} was incubated in a 20 mM Tris buffer containing 5% Me_2SO (v/v) (pH 7.4, 37 °C, 24 h) with a solid template.

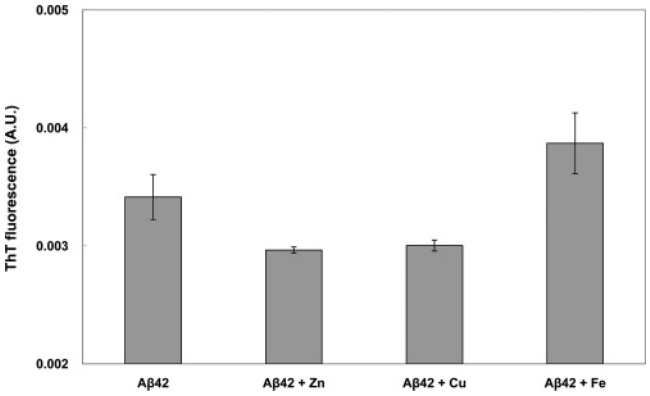

FIGURE 6: ThT fluorescence analysis of Aβ42 deposits induced by different metal ions. A freshly prepared 6 μM Aβ42 solution in the absence or presence of 100 μM Zn^{2+}, Cu^{2+}, or Fe^{3+} was incubated in a 20 mM Tris buffer containing 5% Me_2SO (v/v) (pH 7.4, 37 °C, 24 h) with a solid template.

accelerated by the presence of NaCl when Zn^{2+} (10 μM) was co-incubated with NaCl up to 150 mM concentration. The variance of our results from the work seems to be due to the much higher concentration of Zn^{2+} (100 μM) used in this study. Considering that Zn^{2+} was found at a high concentration of ~1100 μM near the senile plaque deposits according to previous reports (*2*, *5*), the results presented in this study may be more physiologically relevant, but further investigations are needed.

In order to evaluate the effect of metal ions on Aβ42 deposit formation in a quantitative way, AFM images in Figure 1 were analyzed in terms of height and frequency using SPIP software. According to Figure 4, the addition of metal ions into the solution increased the amounts of Aβ deposits that formed on the template surface in the order of $Cu^{2+} < Zn^{2+} < Fe^{3+}$, which were indicated by the shift of Gaussian curves to higher values. By summing the total area under each Gaussian curve in Figure 4, we measured the total volume of Aβ42 deposits that formed on the template in each case (Figure 4, inset). The overall volume of Aβ42 deposits increased in the presence of metal ions compared to the control experiment, which was performed without any metal ions in the solution phase.

Those results show that Fe^{3+} can accelerate the deposition of fibrillar amyloid plaques in AD among the metal ions.

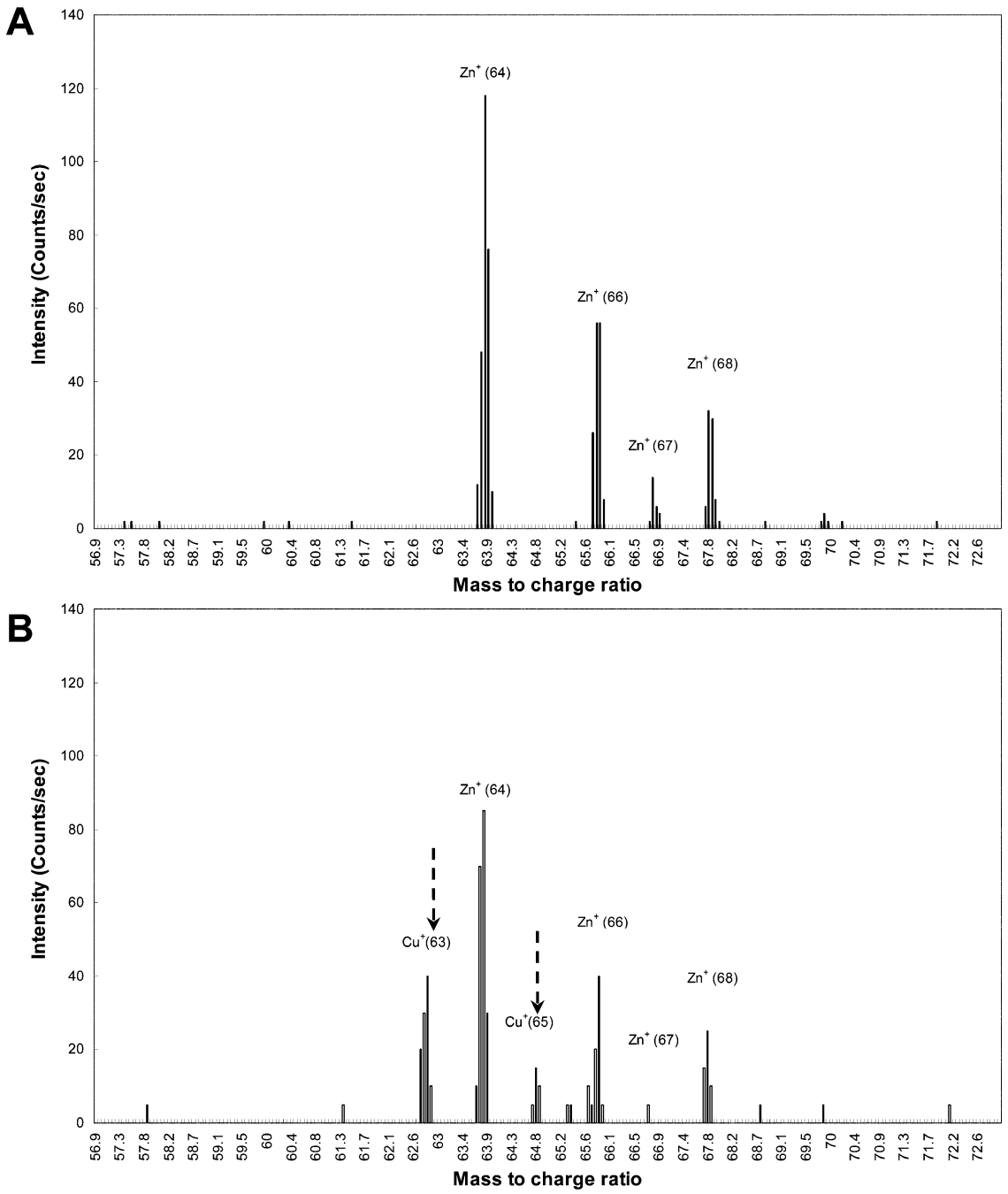

FIGURE 7: Comparison of a SIMS analysis of a plain glass and Cu^{2+}-induced Aβ42 deposits. (A) SIMS spectra of a plain glass. (B) SIMS spectra of Cu^{2+}-induced Aβ42 deposits. Cu^{2+}-induced Aβ42 deposits were formed after 24 h incubation of a solid template in freshly prepared Aβ42 (10 μM) containing 1 mM Cu^{2+}.

According to Maynard et al. (*13*), the concentration of Fe^{3+} within the core and periphery of senile plaque deposits increases with a person's age. Their observations suggest that the concentration of Fe^{3+} may be an important factor in the formation of fibrillar amyloid plaques in vivo. On the contrary, Zn^{2+} and Cu^{2+} increased the rate of Aβ deposition, but mostly only in an amorphous morphology. According to previous studies, the binding of Aβ to Cu^{2+} or Zn^{2+}, which was mediated by histidine residues in positions 13 and 14, accelerated the aggregate formation of Aβ (*14, 15*). However, according to our results, Zn^{2+}-Aβ or Cu^{2+}-Aβ aggregates may not be central mediators to induce fibrillar amyloid plaques. These observations are supported by previous in vitro Aβ aggregation studies. For example, Aβ bound to Zn^{2+} maintained its original conformation without the transition into a thermodynamically irreversible β-sheet conformation (*12*). Furthermore, Cu^{2+}-induced aggregates were reported to be fully reversible by the repeated change between pH 7.4 and pH 6.6, indicating the lack of cross-β-sheet structure (*14*).

FT-IR and ThT Fluorescence Analysis of Aβ42 Aggregates Induced by Metal Ions. The secondary structure of deposits formed on a solid template was analyzed by FT-IR spectroscopy. Figure 5 shows FT-IR spectra of Aβ42 plaques grown on the template in the presence or absence of metal ions. A spectrum of the Aβ42 aggregates formed in the presence of Fe^{3+} clearly shows an amide I band with a relatively strong absorption peak at 1632 cm^{-1}, which

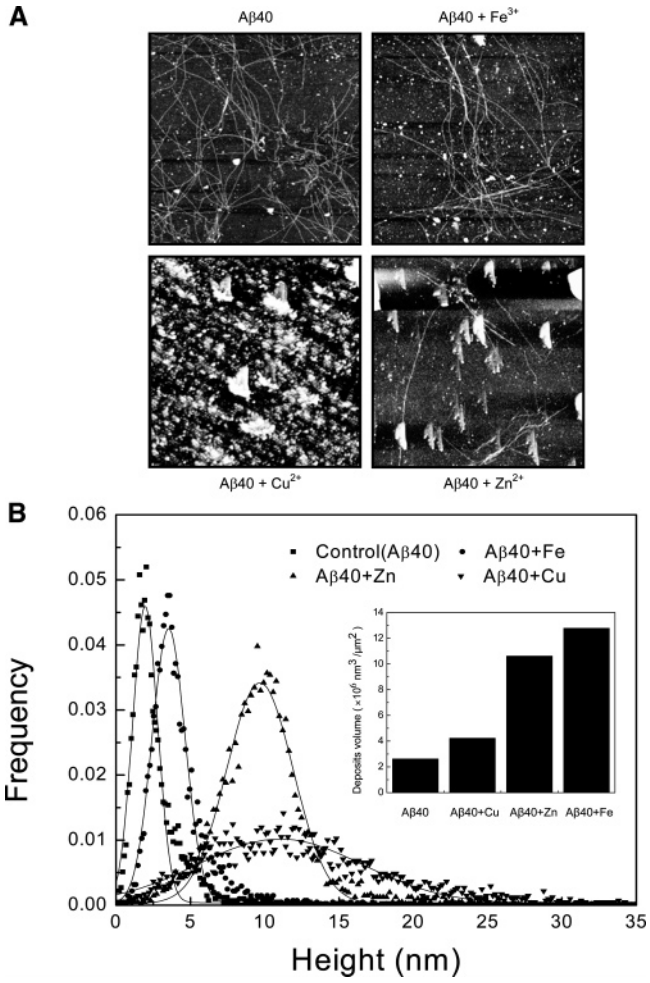

FIGURE 8: Effect of metal ions of amyloid plaque growth with Aβ40. (A) Representative AFM images of Aβ40 deposits on the solid template in the presence or absence of different metal ions. A solid template was incubated in a freshly prepared 30 μM Aβ40 solution with no metal ions, 100 μM Zn^{2+}, 100 μM Cu^{2+}, or 100 μM Fe^{3+}. (B) Quantitative analysis of AFM images as a function of aggregate thickness (i.e., height) and frequency. Inset: Total volume of Aβ40 deposits without metal ions or Aβ40 deposits mediated by different metal ions on the solid surface. The template was prepared by immobilizing 12 h preincubated Aβ40 (30 μM) in a pH 7.4 PBS buffer containing 5% Me_2SO (v/v) on an NHS-activated solid surface. The size of each AFM image is 5 × 5 μm.

indicates the presence of a dominant cross-β-sheet structure in the amyloid aggregates. According to a previous study (*16*), an absorption spectrum in amide I and II bands is dependent on changes in the secondary structure of Aβ peptides. Aβ42 deposits without any metal ion produced a spectrum with relatively reduced absorption peaks around 1632 cm^{-1}. The predominant amide I peaks at 1652 and 1670 cm^{-1} for Zn^{2+}- or Cu^{2+}-induced Aβ42 deposits are associated with predominant α-helix or random coil structures.

Amyloid aggregates formed with or without metal ions were further characterized with a ThT fluorescence assay. It is known that ThT specially binds with amyloid fibers having a cross-β-sheet structure, giving rise to a new emission maximum around 482 nm (*17*). ThT fluorescence intensity at 482 nm is proportional to the mass of amyloid fibrils. According to Figure 6, the changes in ThT fluorescence intensities at 482 nm are consistent with the results obtained by an ex situ AFM analysis in Figure 1. According

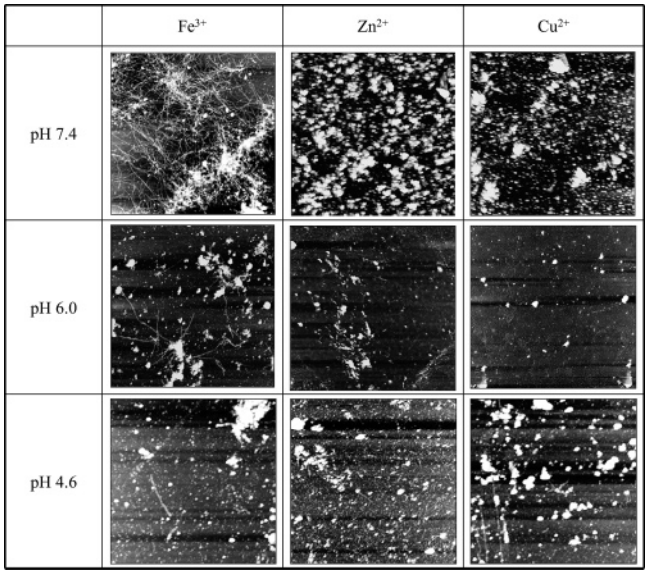

FIGURE 9: Effect of pH on Aβ42 deposition mediated by different metal ions on a solid template. Representative AFM images of Aβ42 deposits on a solid template at pH 7.4, 6.0, or 4.6 in the presence of 100 μM Zn^{2+}, 100 μM Cu^{2+}, or 100 μM Fe^{3+} are shown here. The size of each AFM image is 5 × 5 μm.

to the ThT fluorescence emission patterns, Fe^{3+} accelerated amyloid aggregate growth while Cu^{2+} and Zn^{2+} suppressed amyloid formation.

Detection of Cu Ions within Cu^{2+}-Induced Aβ42 Aggregates Using SIMS Analysis. Secondary ion mass spectroscopy (SIMS) has been widely used to detect unknown secondary ions produced by bombarding a sample with a primary ion beam (*18*, *19*), which has been rarely applied for the study of Aβ plaque deposition. In the present work, we investigated the presence of Cu ions within Aβ42 deposits induced by Cu^{2+} with SIMS in order to confirm whether the binding of a Cu ion to Aβ is associated with the formation of deposits on the solid template. To avoid any nonspecifically adsorbed Cu ions to a sample surface, the samples were extensively cleaned with a phosphate buffer and deionized water. When we analyzed a plain glass that did not have any Aβ42 deposits, the spectrum showed the presence of Zn isotopes at mass-to-charge ratios of 64, 66, 67, and 68 (Figure 7A). In the case of the solid template samples with Cu^{2+}-induced Aβ42 deposits, the peaks for the Cu^{+} isotopes were observed at mass-to-charge ratios of 63 and 65 (Figure 7B). But the detection of Cu^{+} isotopes from Aβ42 deposits induced by the presence of Cu^{2+} may not indicate the reduction of Cu^{2+} to Cu^{+} by Aβ42. Using SIMS, it is not possible to differentiate the existence of either Cu^{+} or Cu^{2+} bound to Aβ42 deposits. According to a previous report (*20*), it was proposed that the reduction of Cu^{2+} to Cu^{+} by Aβ42 may generate H_2O_2, which represents the mechanism of Aβ-mediated oxidative damage in AD. In order to check the possibility of "nonspecifically" bound Cu ions on Aβ42 deposits after through washing, we prepared an Aβ42 deposit sample in the absence of Cu ion, followed by further incubation in Cu ion solution. When we analyzed the surface of the sample with SIMS after washing the sample with buffer solution, we could not observe any peaks responsible for Cu ions (data not shown). The result indicates that nonspecific binding of Cu ion was negligible.

Effect of Metal Ions on Aβ40 Deposition. Although the main components of the earliest detected deposits (called diffuse plaques in vivo) are Aβ42, it is known that fibrillar amyloid plaques are matured by further depositions of the Aβ40 peptide (*1*). In this study, we observed the effect of metal ions on the morphology of Aβ40 deposits using the solid template system. Our results show that both Zn^{2+} and Cu^{2+} disrupt the formation of fibrillar amyloid aggregates regardless of Aβ monomer types (i.e., Aβ40 or Aβ42) (Figure 8A). AFM images indicate that Cu^{2+} is a stronger inducer for amorphous deposits compared to Zn^{2+} (Figure 8A). With the same concentrations of Aβ40 and metal ions, Cu^{2+} completely prevented the formation of fibrillar amyloid plaques compared to Zn^{2+}. The formation of Aβ40 fibrillar amyloid plaques induced by Zn^{2+} might be due to a relatively increased concentration ratio of [Aβ40]/[Zn^{2+}] compared to that of [Aβ42]/[Zn^{2+}]. [Aβ]/[metal ion] concentration ratios may be important to induce the formation of fibrillar amyloid plaques. In addition, a quantitative analysis of AFM images in terms of height and frequency shows that Cu^{2+} and Zn^{2+} were able to accelerate Aβ40 deposition (Figure 8B). Calculated volumes of different Aβ40 deposits that formed on a solid template also indicated relatively higher amounts of Aβ40 deposit formation in the presence of Cu^{2+} or Zn^{2+} compared to Aβ40 alone (Figure 8B, inset).

Effect of pH on Aβ42 Deposition Induced by Metal Ions. It is known that a slightly acidic pH influences the generation of Aβ triggered by the abnormal processing of the amyloid precursor protein (APP) (*21*). Also, pH is considered an important environmental factor affecting the conformational change of Aβ peptides (*22*). Here, we characterized the morphology of Aβ42 aggregates formed on a solid template incubated at pH 7.4, 6.0, or 4.6 in the presence of different metal ions. AFM images (Figure 9) show a considerable difference between amyloid aggregates formed at neutral pH (7.4) and mildly acidic pHs (6.0, 4.6) in the presence of metal ion, especially Fe^{3+}. It was revealed that lowering the solution pH from pH 7.4 to pH 6.0 or 4.6 caused the substantial reduction of Fe^{3+}-induced fibrillar aggregates, resulting in the formation of mostly nonfibrillar deposits. Furthermore, the mildly acidic pHs were not effective in inducing the formation of fibrillar amyloid plaques in the presence of Cu^{2+} or Zn^{2+} (Figure 9). These results suggest that a low pH environment may not be favorable for the formation of fibrillar amyloid plaques in the presence of metal ions.

According to Miura et al. (*23*), metal binding modes of Aβ are pH dependent. They suggested that insoluble aggregates of Cu^{2+}-Aβ can form in mildly acidic conditions (pH ∼6), but not at pH 7.4. Mildly acidic conditions in vivo (pH ∼6) take place in an aged brain and in response to inflammation (*24*). A previous in vitro study reported that Aβ aggregation was markedly accelerated at slightly acidic conditions ($6.5 < pH < 7.0$) in the presence of Cu^{2+}, and the biggest differential in Aβ aggregation was observed at pH 7.4 in the case of Zn^{2+} (*13*). In our current study, we examined the morphology differences of Aβ aggregates formed on a solid template incubated at different pHs in the presence or absence of metal ions. Our results show that the formation and deposition of the fibrillar Aβ42 aggregate was suppressed at mildly acidic pHs of 4.6 and 6.0 in the presence of any metal ion tested in this work. Further investigations are needed to determine environmental factors to change Cu^{2+}- or Zn^{2+}-induced amorphous aggregates into fibrillar amyloid plaques.

In conclusion, our work shows that Cu^{2+} and Zn^{2+} may not be key elements to accelerate the formation and deposition of Aβ fibrillar plaques in both neutral and mildly acidic pH conditions. These metal ions may interfere with β-sheet formation via their binding to Aβ peptides. In contrast, the interaction between Fe^{3+} and Aβ at a pH of 7.4 increased the amounts of fibrillar amyloid plaques. According to recent works (*25*−*27*), diffuse aggregates have higher neurotoxicity than fully grown amyloid fibrils. Considering those reports, the formation of Cu^{2+}- or Zn^{2+}-induced amorphous Aβ aggregates observed in this study may have a relevance to AD pathology. Also, further studies on the effects of multiple metal ions or the sequential treatment of metal ions on Aβ deposition are expected to elucidate the possible role of metal ions in the formation of amyloid plaques in vivo.

REFERENCES

1. Selkoe, D. J. (2001) Alzheimer's disease: Genes, proteins, and therapy, *Physiol. Rev. 81*, 741−766.
2. Bush, A. I. (2003) The metallobiology of Alzheimer's disease, *Trends Neurosci. 26*, 207−214.
3. Bush, A. I., and Tanzi, R. E. (2002) The galvanization of β-amyloid in Alzheimer's disease, *Proc. Natl. Acad. Sci. U.S.A. 99*, 7317−7319.
4. Perry, G., Sayre, L. M., Atwood, C. S., Castellani, R. J., Cash, A. D., Rottkamp, C. A., and Smith, M. A. (2002) The role of iron and copper in the aetiology of neurodegenerative disorders, *CNS Drugs 16*, 339−352.
5. Lovell, M. A., Robertson, J. D., Teesdale, W. J., Campbell, J. L., and Markesbery, W. R. (1998) Copper, iron and zinc in Alzheimer's disease senile plaques, *J. Neurol. Sci. 158*, 47−52.
6. Esler, W. P., Stimson, E. R., Ghilardi, J. R., Felix, A. M., Lu, Y.-A., Vinters, H. V., Mantyh, P. W., and Maggio, J. E. (1997) Aβ deposition inhibitor screen using synthetic amyloid, *Nat. Biotechnol. 15*, 258−263.
7. Kowalewski, T., and Holtzman, D. M. (1999) *In situ* atomic force microscopy study of Alzheimer's β-amyloid peptide on different substrates: New insights into mechanism of β-sheet formation, *Proc. Natl. Acad. Sci. U.S.A. 96*, 3688−3693.
8. Zhu, M., Souillac, P. O., Ionescu-Zanetti, C., Carter, S. A., and Fink, A. L. (2002) Surface-catalyzed amyloid fibril formation, *J. Biol. Chem. 277*, 50914−50922.
9. Kawai, M., Kalaria, R. N., Cras, P., Siedlak, S. L., Velasco, M. E., Shelton, E. R., Chan, H. W., Greenberg, B. D., and Perry, G. (1993) Degeneration of vascular muscle cells in cerebral amyloid angiopathy of Alzheimer disease, *Brain Res. 623*, 142−146.
10. Kokubo, H., Saido, T. C., Iwata, N., Helms, J. B., Shinohara, R., and Yamaguchi, H. (2005) Part of membrane-bound Aβ exists in rafts within senile plaques in Tg2576 mouse brain, *Neurobiol. Aging 26*, 409−418.
11. Ha, C., and Park, C. B. (2006) *Ex situ* atomic force microscopy analysis of β-amyloid self-assembly and deposition on a synthetic template, *Langmuir 22*, 6977−6985.
12. Huang, X., Atwood, C. S., Moir, R. D., Hartshorn, M. A., Vonsattel, J.-P., Tanzi, R. E., and Bush, A. I. (1997) Zinc-induced Alzheimer's Aβ1−40 aggregation is mediated by conformational factors, *J. Biol. Chem. 272*, 26464−26470.
13. Maynard, C. J., Cappai, R., Volitakis, I., Cherny, R. A., White, A. R., Beyreuther, K., Masters, C. L., Bush, A. I., and Li, Q.-X. (2002) Overexpression of Alzheimer's disease amyloid-β opposes the age-dependent elevations of brain copper and iron, *J. Biol. Chem. 277*, 44670−44676.
14. Atwood, C. S., Moir, R. D., Huang, X., Scarpa, R. C., Bacarra, N. M. E., Romano, D. M., Hartshorn, M. A., Tanzi, R. E., and Bush, A. I. (1998) Dramatic aggregation of Alzheimer Aβ by Cu(II) is induced by conditions representing physiological acidosis, *J. Biol. Chem. 273*, 12817−12826.

15. Liu, S.-T., Howlett, G., and Barrow, C. J. (1999) Histidine-13 is a crucial residue in the zinc ion-induced aggregation of the Aβ peptide of Alzheimer's disease, *Biochemistry 38*, 9373−9378.
16. Lin, S.-Y., and Chu, H.-L. (2003) Fourier transform infrared spectroscopy used to evidence the prevention of β-sheet formation of amyloid β(1−40) peptide by a short amyloid fragment, *Int. J. Biol. Macromol. 32*, 173−177.
17. LeVine, H., III (1993) Thioflavin T interaction with synthetic Alzheimer's disease β-amyloid peptides: detection of amyloid aggregation in solution, *Protein Sci. 2*, 404−410.
18. Chakraborty, B. R., Haranath, D., Chander, H., Hellweg, S., Dambach, S., and Arlinghaus, H. F. (2000) TOF-SIMS and laser-SNMS investigations of dopant distribution in nanophosphors, *Nanotechnology 16*, 1006−1015.
19. Godines, J. A., Villegas, A., Kudriavtsev, Y., Asomoza, R., Morales-Acevedo, A., Escamilla, A., Arriaga, G., Hernández-Contreras, H., Contreras-Puente, G., Vidal, J., Chavarría, M., and Fragoso-Soriano, R. (2004) Comparative secondary ion mass spectroscopy analysis of solar cell structures grown by pulsed laser ablation and ion sputtering, *Semicond. Sci. Technol. 19*, 213−218.
20. Huang, X., Cuajungco, M. P., Atwood, C. S., Hartshorn, M. A., Tyndall, J. D. A., Hanson, G. R., Stokes, K. C., Leopold, M., Multhaup, G., Goldstein, L. E., Scarpa, R. C., Saunders, A. J., Lim, J., Moir, R. D., Glabe, C., Bowden, E. F., Masters, C. L., Fairlie, D. P., Tanzi, R. E., and Bush, A. I. (1999) Cu(II) potentiation of Alzheimer Aβ neurotoxicity, *J. Biol. Chem. 274*, 37111−37116.
21. Selkoe, D. J. (1994) Normal and abnormal biology of the β-amyloid precursor protein, *Annu. Rev. Neurosci. 17*, 489−517.
22. Matsunaga, Y., Îerovnik, E., Yamada, T., and Turk, V. (2002) Conformational changes preceding amyloid-fibril formation of amyloid-beta and stefin B: Parallels in pH dependence, *Curr. Med. Chem. 9*, 1717−1724.
23. Miura, T., Suzuki, K., Kohata, N., and Takeuchi, H. (2000) Metal binding modes of Alzheimer's amyloid β-peptide in insoluble aggregates and soluble complexes, *Biochemistry 39*, 7024−7031.
24. Maynard, C. J., Bush, A. I., Masters, C. L., Cappai, R., and Li, Q.-X. (2005) Metals and amyloid-β in Alzheimer's disease, *Int. J. Exp. Pathol. 86*, 147−159.
25. Dahlgren, K. N., Manelli, A. M., Stine, W. B., Jr., Baker, L. K., Krafft, G. A., and LaDu, M. J. (2002) Oligomeric and fibrillar species of amyloid-β peptides differentially affect neuronal viability, *J. Biol. Chem. 277*, 32046−32053.
26. Gong, Y., Chang, L., Viola, K. L., Lacor, P. N., Lambert, M. P., Finch, C. E., Krafft, G. A., and Klein, W. L. (2003) Alzheimer's disease-affected brain: Presence of oligomeric Aβ ligands (ADDLs) suggests a molecular basis for reversible memory loss, *Proc. Natl. Acad. Sci. U.S.A. 100*, 10417−10422.
27. Kayed, R., Head, E., Thompson, J. L., McIntire, T. M., Milton, S. C., Cotman, C. W., and Glabe, C. G. (2003) Common structure of soluble amyloid oligomers implies common mechanism of pathogenesis, *Science 300*, 486−489.

BI7000032